JOC Article

Bis-morpholine-Substituted Perylene Bisimides: Impact of Isomeric Arrangement on Electrochemical and Spectroelectrochemical Properties

Gudrun Goretzki,[†] E. Stephen Davies,[†] Stephen P. Argent,[†] Wassim Z. Alsindi,[†] Alexander J. Blake,[†] John E. Warren,[‡] Jonathan McMaster,[†] and Neil R. Champness*[,†]

School of Chemistry, University of Nottingham, University Park, Nottingham NG7 2RD, U.K., and Daresbury Laboratory, Synchrotron Radiation Source, Warrington, WA4 4AD Cheshire, England

neil.champness@nottingham.ac.uk

Received July 18, 2008

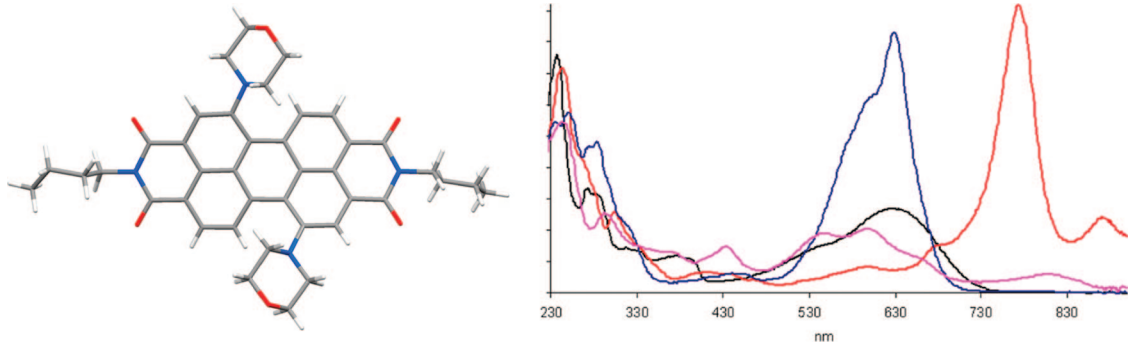

The synthesis and separation of the 1,6- and 1,7- isomers of *N*,*N*′-bis(*n*-butyl)dimorpholino-3,4:9,10-perylenetetracarboxylic acid bisimide are reported. Investigations of the electrochemical and spectroscopic, in particular, spectroelectrochemical, properties of the two isomers reveal a sequence of electrochemically and chemically reversible redox processes for both isomers. Importantly, the 1,7-isomer of *N*,*N*′-bis(*n*-butyl)dimorpholino-3,4:9,10-perylenetetracarboxylic acid bisimide was observed to undergo a two-electron oxidation process, which contrasts with the behavior of both the corresponding 1,6-isomer and other related amino-substituted perylene bis-imide species.

Introduction

3,4:9,10-Perylenetetracarboxylic bisimides and their derivatives are currently receiving a great deal of attention due to their remarkable electrochemical and optical properties.[1] These properties have made such compounds excellent candidates for applications such as *n*-type semiconductors,[1,2] xerographic photoreceptors,[3] thin film-transistors,[4] solar cells,[5] and cell imaging.[6] In addition, their extended aromatic structure and extensive possibilities for derivatization make them attractive targets for the generation of liquid crystals[7] and for surface-based self-assembly processes.[8]

Derivatization of 3,4:9,10-perylenetetracarboxylic bisimides can be achieved by two main approaches. First, the imide functionality can be altered by the facile variation in the amine appendage utilized in the initial formation of the imide moiety. Such functionalization is readily achieved but has limited influence upon the electronic and optical properties of the

[†] University of Nottingham.
[‡] Synchrotron Radiation Source.

(1) Würthner, F. *Chem. Commun.* **2004**, 1564.
(2) (a) Langhals, H. *Heterocylces* **1995**, *40*, 477. (b) Yoo, B.; Jung, T.; Basu, D.; Dodabalapur, A.; Jones, B. A.; Faccetti, A.; Wasielewski, M. R.; Marks, T. J. *Appl. Phys. Lett.* **2006**, *88*, 082104.
(3) Law, K.-Y. *Chem. Rev.* **1993**, *93*, 449.
(4) Horowitz, G.; Kouki, F.; Spearman, P.; Fichou, D.; Nogeus, C.; Pan, X.; Garnier, F. *Adv. Mater.* **1996**, *8*, 224.
(5) Tang, C. W. *Appl. Phys. Lett.* **1986**, *48*, 183.
(6) Qu, J. Q.; Kohl, C.; Pottek, M.; Mullen, K. *Angew. Chem., Int. Ed.* **2004**, *43*, 1528.
(7) Würthner, F.; Thalacker, C.; Diele, S.; Tschierske, C. *Chem.—Eur. J.* **2001**, *7*, 2245.
(8) (a) Theobald, J. A.; Oxtoby, N. S.; Phillips, M. A.; Champness, N. R.; Beton, P. H. *Nature* **2003**, *424*, 1029. (b) Swarbrick, J. C.; Ma, J.; Theobald, J. A.; Oxtoby, N. S.; O'Shea, J. N.; Champness, N. R.; Beton, P. H. *J. Phys. Chem. B* **2005**, *109*, 12167. (c) Theobald, J. A.; Oxtoby, N. S.; Champness, N. R.; Beton, P. H.; Dennis, T. J. S. *Langmuir* **2005**, *21*, 2038. (d) Perdigão, L. M. A.; Perkins, E. W.; Ma, J.; Staniec, P. A.; Rogers, B. L.; Champness, N. R.; Beton, P. H. *J. Phys. Chem. B* **2006**, *110*, 12539. (e) de Feyter, S.; Miura, A.; Yao, S.; Chen, Z.; Würthner, F.; Jonkheijm, P.; Schenning, A.P. H. J.; Meijer, E. W.; de Schryver, F. C. *Nano Lett.* **2005**, *5*, 77.

10.1021/jo801557e CCC: $40.75
Published on Web 10/15/2008

aromatic perylene core.[9] Alternatively, derivatization can be achieved in the "bay region" in the 1, 6, 7, and/or 12 positions of the perylene core. Such reactions have been widely exploited via the formation of halogenated 3,4:9,10-perylenetetracarboxylic bisimide species and subsequent substitution of the halide groups with a variety of chemical functionalities.[1] Of the possible derivatives that could be produced, the most commonly studied species are the family of tetrasubstituted compounds that tend to have increased solubility characteristics and, importantly, do not exhibit isomeric arrangements in the perylene "bay region".[1,10]

The next most studied group of compounds is the disubstituted species that exhibit isomerism with both 1,6- and 1,7-isomers potentially being formed. Disubstituted 1,6- and 1,7-*N*,*N*′-bis(*n*-alkyl)-3,4:9,10-perylenetetracarboxylic bisimides are prepared from the reaction of a chosen nucleophile with the "as synthesized" *N*,*N*′-bis(*n*-alkyl)dibromo-3,4:9,10-perylenetetracarboxylic bisimide.[11−15] It has been noticed previously that the preparation of *N*,*N*′-bis(*n*-alkyl)dibromo-3,4:9,10-perylenetetracarboxylic bisimides yields a mixture of 1,7- and 1,6-isomers in an estimated 4:1 ratio.[11] However, substitution of the bromo substitutents can lead to disubstituted perylene bisimide products that may, in selected cases, be separated by column chromatography. As the 1,7-isomer is always the major product from the bromination of perylene-3,4:9,10-tetracarboxylic acid, the same isomer is also the major product from substitution reactions using the "as synthesized" *N*,*N*′-bis(*n*-alkyl)-dibromo-3,4:9,10-perylenetetracarboxylic bisimide. As a result, the vast majority of disubstituted perylenetetracarboxylic bisimides that have been reported and studied are 1,7-isomers.

It has been noted that the electrochemical and optical properties of the 1,6- and 1,7-isomers differ significantly where the bay region substituent is *n*-octylamino.[13] Here, we report the synthesis and separation of the 1,6- (**1a**) and 1,7- (**1b**) isomers of *N*,*N*′-bis(*n*-butyl)-dimorpholino-3,4:9,10-perylenetetracarboxylic acid bisimide and subsequent investigations of the electrochemical and spectroscopic, in particular spectroelectrochemical, properties of the two isomers. Notable differences are observed between the two tertiary amine morpholine isomers and in comparison to analogous secondary amine *n*-octylamino-based species.[13] Although morpholine-substituted perylene-bisimides have been reported previously with a range of different appendages attached to the imide nitrogen atom and used for a variety of different applications,[14,15] this study represents the first time that the redox properties of such systems have been extensively investigated.

SCHEME 1. *N*,*N*′-Di(*n*-butyl)-1,6-dimorpholino-3,4,9,10-tetracarboxylic Acid Bisimide 1a and *N*,*N*′-di(*n*-butyl)-1,7-dimorpholino-3,4,9,10-tetracarboxylic Acid Bisimide 1b

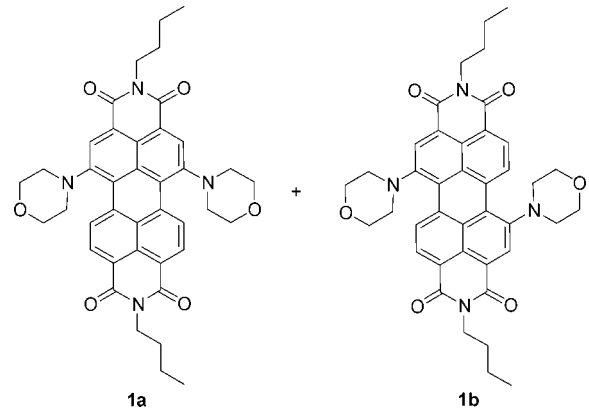

Results and Discussion

Synthesis. *N*,*N*′-Bis(*n*-butyl)-1,6-dimorpholino-3,4:9,10-perylenetetracarboxylic acid bisimide **1a** and *N*,*N*′-di(*n*-butyl)-1,7-dimorpholino-3,4:9,10-perylenetetracarboxylic acid bisimide **1b** (Scheme 1) were prepared by morpholine substitution of "as synthesized" *N*,*N*′-bis(*n*-butyl)-dibromo-3,4:9,10-perylenetetracarboxylic bisimide using morpholine as both reagent and solvent.[11]

Single crystals of **1b** were grown by diffusion of hexane vapor into a solution of **1b** in $CHCl_3$. An X-ray structural determination revealed the conformational arrangement of the molecule in the solid state. As is anticipated for 1,7-disubstituted perylenetetracarboxylic bisimides, the molecule adopts a twisted arrangement of the perylene core induced by steric interactions between the morpholinyl substituents and the proton located on the adjacent position (i.e., position 12- or 6- for the 1- and 7-morpholinyl substituents, respectively). Thus, the perylene core can be considered as two naphthyl moieties linked along the C13−C14 and C17−C18 bonds. The dihedral angles between the two naphthyl subunits in the two independent molecules in the crystallographic asymmetric unit are 21.9 and 26.0° (Figure 1). The morpholinyl subunits both adopt a chair conformation and are positioned such that both lie on the same face of the perylene core of the molecule. Attempts to grow single crystals of **1a** proved unsuccessful.

Electrochemical and Optical Spectroscopy Investigations. The electrochemical behavior of **1a** and **1b** in CH_2Cl_2 solution was investigated by cyclic voltammetry, coulometry, EPR spectroscopy, and UV/vis spectroelectrochemistry in order to establish the comparative behavior of the two isomers. Electrochemical data are summarized in Table 1, and full details of methods and spectroscopic data can be found in the Supporting Information.

Reduction Processes of 1a and 1b. Cyclic voltammetric investigations of **1a** and **1b** reveal two one-electron reduction processes that are both electrochemically and chemically reversible (Figure 2) by cyclic voltammetry over a scan rate range 0.02−0.3 V s^{-1} and by UV/vis spectroelectrochemistry at 273 K, respectively (see below). The reductions observed for **1a** and **1b** follow the trends reported for other perylenetetracarboxylic bisimide compounds.[1,13−15] The half-wave potentials of these reductions, taken from cyclic voltammetry, are essentially the same for each isomer (**1a** −1.11 and −1.29 V; **1b** −1.11 and −1.30 V) and match exactly with results from

(9) Langhals, H.; Demmig, S.; Huber, H. *Spectrochim. Acta* **1988**, *44a*, 189.
(10) (a) Flamigni, L.; Ventura, B.; You, C.-C.; Hippius, C.; Würthner, F. *J. Phys. Chem. C* **2007**, *111*, 622. (b) Beckers, E. H. A.; Chen, Z.; Meskers, S. C. J.; Jonkheijm, P.; Schenning, A. P. H. J.; Li, X.-Q.; Osswald, P.; Würthner, F.; Janssen, R. A. J. *J. Phys. Chem. B* **2006**, *110*, 16967. (c) Iden, R.;Seybolf,G. (BASF AG) Ger. Pat. Appl. DE 3434059 A1, 1985; *Chem. Abstr*. **1985**, *103*, 38696q.
(11) Würthner, F.; Stepanenko, V.; Chen, Z.; Saha-Möller, C. R.; Kocher, N.; Stalke, D. *J. Org. Chem.* **2004**, *69*, 7933.
(12) Nolde, F.; Pisula, W.; Mueller, S.; Kohl, C.; Müllen, K. *Chem. Mater.* **2006**, *18*, 3715.
(13) Ahrens, M. J.; Tauber, M. J.; Wasielewski, M. R. *J. Org. Chem.* **2006**, *71*, 2107–2114.
(14) (a) Fan, L.; Xu, Y.; Tian, H. *Tetrahedron Lett.* **2005**, *46*, 4443–4447. (b) Yukruk, F.; Dogan, A. L.; Canpinar, H.; Guc, D.; Akkaya, E. U. *Org. Lett.* **2005**, *7*, 2885–2887. (c) Sugiyasu, K.; Fujita, N.; Shinkai, S. *Angew. Chem., Int. Ed.* **1994**, *43*, 1229–1233. (d) Franceschin, M.; Alvino, A.; Ortaggi, G.; Bianco, A. *Tetrahedron Lett.* **2004**, *45*, 9015–9020.
(15) Zhao, Y.; Wasielewski, M. R. *Tetrahedron Lett.* **1999**, *40*, 7047–7050.

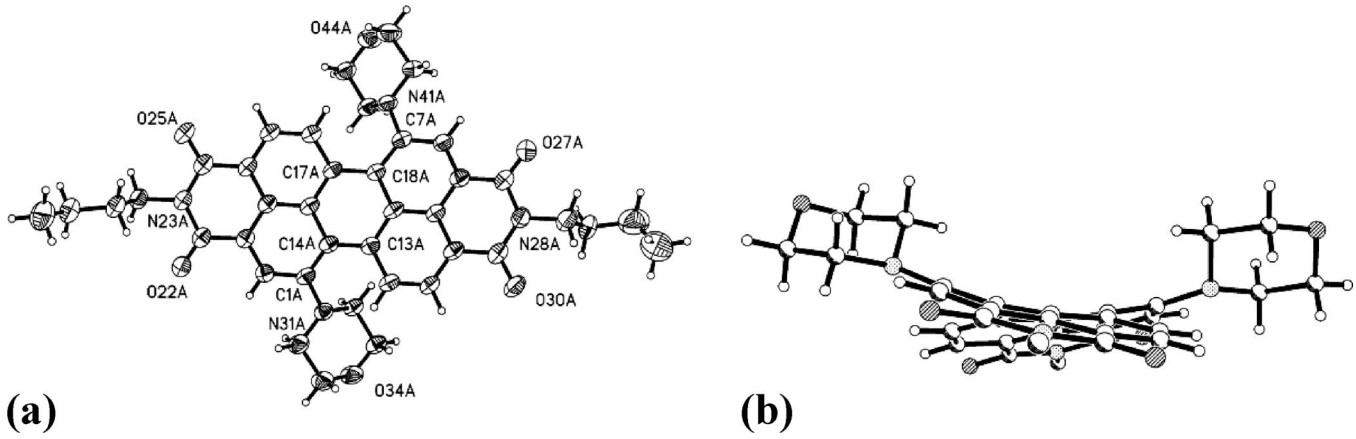

FIGURE 1. View of single-crystal X-ray structure of **1b** showing (a) the numbering scheme used and illustrating (b) the twist observed between the two naphthyl subunits of the central perylene core. Displacement ellipsoids in (a) are drawn at the 50% probability level.

TABLE 1. Electrochemical Data for Disubstituted *N,N′*-Bis(*n*-butyl)-3,4:9,10-perylene Tetracarboxylic Bisimides[a]

compd	first reduction	second reduction	first oxidation	second oxidation	ΔE (Fc^+/Fc)
		Cyclic Voltammetry Data			
1a	−1.11 (0.07)	−1.30 (0.07)	+0.59 (0.07) [b]	+0.94 (0.06)	(0.07)
1b	−1.11 (0.07)	−1.29 (0.07)	+0.43 (0.05)		(0.07)
2 di-Br	−0.90 (0.07)	−1.08 (0.07)			(0.07)
3a[c]	−1.32	−1.51	+0.44	+0.59	
3b[c]	−1.31	−1.48	+0.29	+0.48	
		Square Wave Voltammetry Data			
1a	−1.11	−1.30	+0.59	+0.95	
1b	−1.11	−1.29	+0.43		
2 di-Br	−0.90	−1.08			

[a] All potentials reported as $E_{1/2}$ (= (E_p^a + E_p^c)/2) in V vs Fc^+/Fc at 0.1 V s^{-1} scan rate and quoted to the nearest 0.01 V. Values in parentheses are ΔE (= E_p^a − E_p^c) for the couple at 0.01 Vs^{-1}. [b] Further oxidation at E_p^a 0.91 V. [c] From ref 13.

square wave voltammetry. Notably, the reduction potentials are considerably more negative than those for the dibromo precursors **2** (−0.90 and −1.08 V vs Fc^+/Fc), demonstrating that the reduction processes are insensitive to the position (1,7 versus 1,6) of the *N*-morpholinyl moiety but are sensitive to the electron-withdrawing/donating nature of the appended group, contrasting sharply with trends observed for the oxidations of **1a** and **1b** (see below). The potential of the first reduction process for **1b** is highly similar to those observed for 1,7-bis(*N*-morpholinyl)-*N,N′*-di-cyclohexyl-3,4:9,10-perylenetetracarboxylic acid bisimide and other related *N,N-R*-3,4:9,10-perylenetetracarboxylic acid bisimides with alternative substitution at the imide nitrogen atom.[15] Comparison of reduction potentials for two secondary amines appended at the 1,7 positions, *N*-morpholinyl in **1b** and *N*-pyrrolidinyl in 1,7-bis(*N*-pyrrolidinyl)-*N,N*-dicyclohexyl-3,4:9,10-perylenetetracarboxylic acid bisimide (−1.28 and −1.46 V vs Fc^+/Fc), shows *N*-pyrrolidinyl to be more effective at donating electron density into the π-system.[16]

The first reduction of **1a** and **1b** was confirmed as a one-electron process by coulometry and gave green and turquoise solutions, respectively. These solutions are EPR active and gave signals consistent with generation of the radical anions, $\mathbf{1a}^{\bullet-}$ (g_{iso} 2.0036, ΔB_{p-p} = 4.0 G) and $\mathbf{1b}^{\bullet-}$ (g_{iso} 2.0034, ΔB_{p-p} = 4.1 G). Hyperfine splittings were not observed, a result that is consistent with the EPR spectrum reported for [1,7-bis(3,5-di-*tert*-butylphenoxy)-*N,N*-di-2-ethylhexyl-3,4:9,10-perylenetetracarboxylic acid bisimide]$^{\bullet-}$, formed by photoreduction of the parent molecule in the presence of triethylamine.[17] The second reduction of **1a** and **1b** is also a one electron process and yields the dianions, both of which are dark blue. These solutions are essentially EPR silent, with only residual signals (<8% relative to $\mathbf{1a}^{\bullet-}$ and $\mathbf{1b}^{\bullet-}$) present.

The in situ one- and two-electron reductions of **1a** (Figure 3) and **1b** (Figure 4) were followed by UV/vis/nIR spectroelectrochemistry at an optically transparent electrode. The one-electron reduced radical anions show bands which are red-shifted relative to their parent molecules, with a series of transitions extending into the nIR region; a considerable enhancement in measured extinction coefficients ($[1,7]^{\bullet-}$(λ_{max} 786 nm, ϵ 83000); $[1,6]^{\bullet-}$(λ_{max} 774 nm, ϵ 90000)) relative to the neutral molecules is also observed, results that are consistent with data reported previously.[17] The second reduction blue-shifts the spectra with respect to those of the radical anion, with the most intense transition for both $\mathbf{1a}^{2-}$ (λ_{max} 630 nm, ϵ 82000) and $\mathbf{1b}^{2-}$ (λ_{max} 626 nm, ϵ 72000) occurring at similar wavelength.

The above results are consistent with the two-step reduction mechanism proposed for perylene bisimide molecules in which the majority of electron density is localized at the carbonyl oxygens.[18] This mechanism predicts both the close similarity in redox potentials and the observation that the first reduction generates a radical anion while the addition of a second electron gives the dianion in which a semiquinoidal configuration is adopted in a longitudinal fashion through half of the perylenebis(dicarboximide) core, thereby accounting for both the similarity in UV/vis spectra of $\mathbf{1a}^{2-}$ and $\mathbf{1b}^{2-}$ and the diminished EPR signals.

Oxidation Processes of 1a and 1b. In contrast to the reduction processes, electrochemical oxidation discriminates between the [1,6] and [1,7] isomers: the [1,6] isomer **1a** undergoes an electrochemically reversible one-electron oxidation (by coulometry) at $E_{1/2}$ 0.59 V vs Fc^+/Fc, at ambient temperature and with scan rates of 0.02−0.3 V s^{-1}. Two additional oxidation processes, at E_p^a 0.91 and $E_{1/2}$ 0.94 V, were also observed (Figure 2a), but these were not investigated further.

The first oxidation process ($E_{1/2}$ 0.59 V vs Fc^+/Fc) was found to be chemically reversible by UV/vis spectroelectrochemistry

(16) Lukas, A. S.; Zhao, Y.; Miller, S. E.; Wasielewski, M. R. *J. Phys Chem. B* **2002**, *106*, 1299–1306.

(17) Tauber, M. J.; Kelley, R. F.; Giaimo, J. M.; Rybtchinski, B.; Wasielewski, M. R. *J. Am. Chem. Soc.* **2006**, *128*, 1782–1783.

(18) Lee, S. K.; Zu, Y.; Herrmann, A.; Geerts, Y.; Müllen, K.; Bard, A. J. *J. Am. Chem. Soc.* **1999**, *121*, 3513–3520.

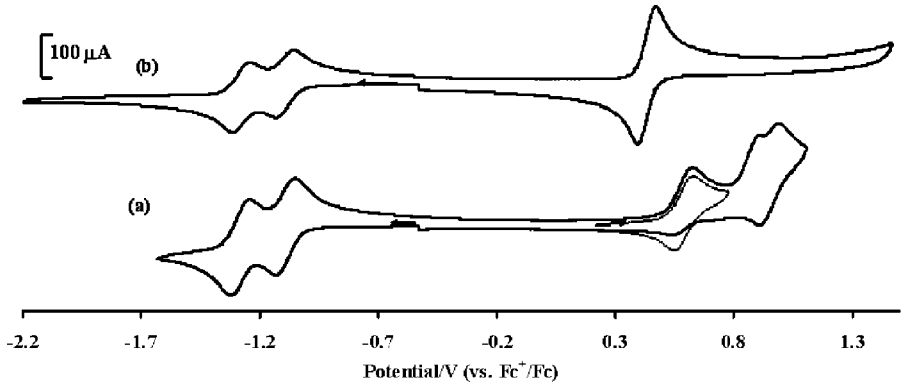

FIGURE 2. Cyclic voltammograms recorded in CH_2Cl_2 for (a) **1a** (the 1,6-isomer) and (b) **1b** (the 1,7-isomer). Note the different oxidation behavior exhibited by the two isomers.

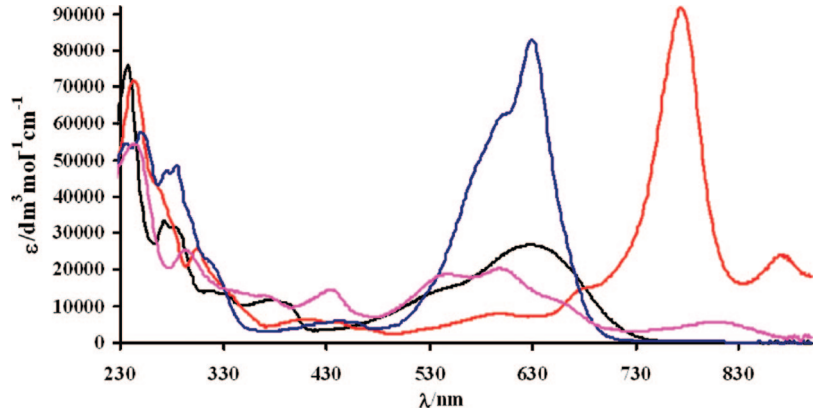

FIGURE 3. UV−vis spectra recorded in CH_2Cl_2 using spectroelectrochemical methods for **1a**. The spectra are identified as follows: **1a**, black; $\mathbf{1a}^{\bullet-}$, red; $\mathbf{1a}^{2-}$, blue; oxidized species $\mathbf{1a}^{+}$ (magenta).

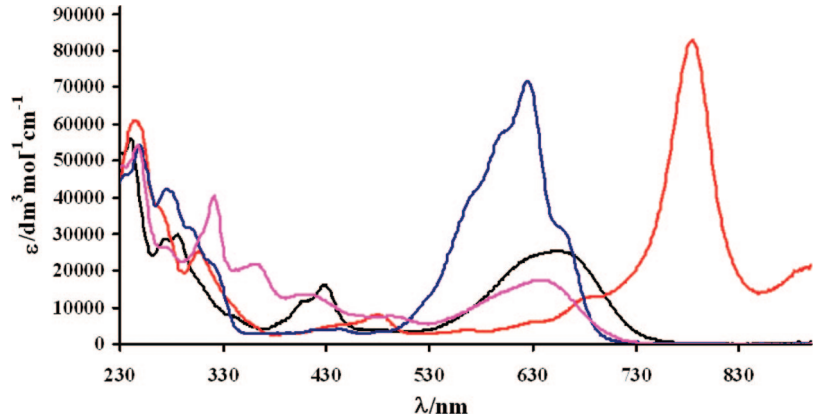

FIGURE 4. UV−vis spectra recorded in CH_2Cl_2 using spectroelectrochemical methods for **1b**. The spectra are identified as follows: **1b**, black; $\mathbf{1b}^{\bullet-}$, red; $\mathbf{1b}^{2-}$, blue; oxidized species $\mathbf{1b}^{2+}$ (magenta).

at 228 K. A small difference, maximum ca. 4%, was observed between the intensity of the initial spectrum compared with that produced after the redox cycle, although no new bands were apparent. Solutions of the one-electron oxidized **1a**, electrochemically generated and maintained at or below 233 K, were found to be EPR active (g_{iso} = 2.0032, ΔB_{p-p} = 13.5 G), consistent with the formation of a radical cation species, $\mathbf{1a}^{\bullet+}$, as noted for one-electron oxidized 1,6-bis(*n*-octylamino)-3,4:9,10-perylenetetracarboxylic acid bisimide (g_{iso} = 2.0025). Small hyperfine couplings were observed that were obscured by line width. Attempts to better resolve the splittings by recording spectra at higher temperatures resulted in the loss of EPR activity and was attributed to the decay of $\mathbf{1a}^{\bullet+}$. This was consistent with the results from cyclic voltammetry, recorded at ambient temperature, of oxidized solutions of **1a** which showed depletion of current intensity for the $[1,6]^{+/0}$ couple and the development of new redox processes at negative potential. These processes were not studied further. The thermal instability of $\mathbf{1a}^{+}$ is in stark contrast to reports of one-electron oxidized 1,6-bis(*n*-octylamino)perylene-3,4:9,10-perylenetetracarboxylic acid bisimide, which is stable at room temperature for some considerable time. The reasons for such a difference are unclear, especially given that deprotonation of the amine, a known mode of decay, is not accessible for morpholino-substituted perylenes.

Changes in the UV/vis spectra upon oxidation of **1a** were followed by spectroelectrochemistry at 228 K. Oxidation

resulted in the generation of a spectrum in which absorption extended, unbroken, through the visible region and into the nIR (Figure 3), the result of a series of closely overlapping transitions. However, unlike spectra recorded for the corresponding reduced species, none of these bands had an extinction coefficient greater than that of the parent molecule, possibly indicative of a poorer overlap between morpholinyl and perylene orbitals upon oxidation. This result is consistent with data reported for one-electron oxidized 1,7-bis(N-pyrrolidinyl)-*N*,*N*-dicyclohexyl-3,4:9,10-perylenetetracarboxylic acid bisimide.[16]

The oxidation of the [1,7] isomer, **1b**, is a two-electron process (by coulometry). This contrasts with the oxidation of the [1,6] isomer, **1a**, and data reported in literature for oxidations of other 1,7-substituted perylenetetracarboxylic acid bisimide compounds.[1,13−16] The oxidation of **1b** occurs at $E_{1/2}$ 0.43 V vs Fc^+/Fc, a potential 0.16 V less positive than the one-electron oxidation of **1a**.

The results of cyclic voltammetry, at ambient temperature, for the $\mathbf{1b}^{2+/0}$ couple showed peak currents were proportional to the square root of scan rate (anodic, $R^2 = 1.000$; cathodic, $R^2 = 0.999$) and the ratio I_p^c/I_p^a was ca. 0.9 across the scan rate range ($0.02 - 1$ Vs^{-1}) with no significant variation. Additionally, ΔE ($= E_p^a - E_p^c$) of 0.05 V was found to be less than ΔE for the Fc^+/Fc couple (0.07 V), used as the internal standard. Although ΔE for the $\mathbf{1b}^{2+/0}$ couple showed slight scan rate dependence (50−70 mV between 0.02−1 V s^{-1}), this was comparable to the variation in ΔE for the Fc^+/Fc couple (70−90 mV) under identical conditions—this variation is consistent with the effect of operating in a solvent (CH_2Cl_2) of low dielectric constant. Hence, the $\mathbf{1b}^{2+/0}$ couple is assigned tentatively to an EE process whereby the oxidation occurs on two equivalent orbitals within the molecule. These groups interact attractively [$\Delta E°$ ($= E_{ox1} - E_{ox2}$) > 35.6 mV] resulting in the second oxidative process becoming easier after the first oxidation. Such processes typically require a large structural rearrangement, or a large solvation effect or ion pairing as a result of the first electron transfer step.[19]

The oxidation of **1b** was shown to be chemically reversible only at 233 K by spectroelectrochemistry. This experiment showed the growth and subsequent disappearance of absorption bands, most noticeably in the nIR region (ca. 830 nm cf. $[1,6]^{\bullet+}$) (Figure 4) and an absence of isosbestic points. This behavior contrasts with the reductions of **1b** and both oxidation and reductions of **1a** in which the progress of redox interconversion was manifest as successive spectra interchanging smoothly through a series of isosbestic points. The cyclic voltammetry of **1a**, at 233 K and 0.1 V s^{-1} in CH_2Cl_2, showed no evidence for the separation of the $\mathbf{1b}^{2+/0}$ couple into two components. However, repeating the measurements in either DMF or MeCN resulted in a change in the nature of the electron-transfer process for the oxidation of **1b**, with a shoulder appearing on the high potential side of the oxidation wave, accompanied by a single wave in the reduction half-cycle.

The EPR spectrum (at 243 K) of the electrogenerated two-electron oxidized $[1,7]^{2+}$, i.e., $[\mathbf{1b}]^{2+}$, is essentially silent. A structured ($g_{iso} = 2.0035$) signal was observed, but spin quantification of this signal versus a known concentration of the stable radical DPPH showed it to represent ca. 4% of the expected spin for one unpaired electron. Hence, the first oxidation of **1b** involves the transfer of two electrons and yields a dication possibly involving the spin-pairing of electrons and contrasts with the generation of an EPR active radical cation, $\mathbf{1a}^{\bullet+}$, from the first, one-electron oxidation of **1a**.

In summary, although both **1a** and **1b** show highly similar reduction behavior, the oxidation processes associated with the two compounds are quite distinct. Whereas the [1,6] isomer, **1a**, undergoes well-separated oxidation processes, the first of which was shown to be one electron, the [1,7] isomer, **1b**, undergoes a single two-electron process leading to a dicationic species.

Comparison between 1a/1b and 1,6- (3a) and 1,7-Bis(*n*-octylamino)perylene-3,4:9,10-bis(dicarboximide) 3b. A particularly useful comparison can be drawn between the electrochemical properties of **1a** and **1b**, tertiary amine substituted perylene bisimides, and the related secondary amine substituted species 1,6-bis(*n*-octylamino)-3,4:9,10-perylenetetracarboxylic acid bisimide **3a** and 1,7-bis(*n*-octylamino)-3,4:9,10-perylenetetracarboxylic acid bisimide **3b**.[13]

The clearest comparison can be seen from the relative positions of the redox processes observed for all four molecules (Table 1). The effect of replacing the tertiary amine morpholinyl substituents with secondary amine (*n*-octylamino) appendages is to shift the energy manifold such that **3a** and **3b** are more difficult to reduce but easier to oxidize than **1a** and **1b**. Thus, the difference between the first reduction and first oxidation potentials (Δ_{o-r}) is 1.76 and 1.60 V for **3a** and **3b**, respectively, and 1.70 and 1.54 V for **1a** and **1b**, respectively, so it may be deduced that a similar orbital manifold operates in both sets of compounds.

Given the similarity in reduction potentials for **1a** and **1b** (and **3a** and **3b**), the difference in properties between these isomers must arise from the nature of the HOMO. In terms of the oxidation processes for **3a/3b** and **1a/1b** the most noticeable difference occurs in the separation between first and second oxidation potentials. For **3a** and **3b** this is sufficient to allow discrete oxidations to occur. This is particularly noticeable for **3b**, the 1,7 isomer, which undergoes two distinct, sequential oxidation processes, in sharp contrast to the behavior of **1b**. In contrast, the behavior of the two 1,6-isomers **1a** and **3a** is similar, with both compounds undergoing a second oxidation processes. For both pairs of compounds, the first oxidation of the 1,6-isomers is more positive than that for the analogous 1,7-isomers.

We carried out restricted DFT calculations at the B3LYP/6-31G* level on models of **1a** and **1b** derived from the X-ray crystal structure of **1b** to provide further qualitative insight into the electronic structures and the trends in reduction and oxidation potentials of these compounds. Both geometry optimized structures show a twist within the perylene core with interplanar angles between the naphthyl subunits of 21.9 and 26.0° for **1a** and **1b**, respectively. The latter angle is in reasonable agreement with the experimentally determined angle (23.9° ave.) for **1b** and is significantly greater than that calculated for **3b** (14.9 °).[13] These results presumably reflect the greater steric demand of the morpholine substituents relative to the *n*-octylamino groups in **3b**. Compounds **1a** and **1b** possess molecular orbital manifolds (Figure 5) similar to one another and to **3a** and **3b**,[13] with LUMOs that are considerably more delocalized across the molecular framework when compared to the HOMOs. Thus, the LUMOs are more localized around the perylene core (Figure

(19) Bard A. J.; Faulkner, L. R. *Electrochemical Methods, Fundamentals and Applications*, 2nd ed.; Wiley: New York, pp 505−507.

5). The relative trends in LUMO and HOMO energies mirror the first reduction and oxidation potentials, respectively, for each species. Thus, the LUMO energies for **1a** and **1b** are identical (−3.075 eV) and lower in energy than the LUMOs of **3a** and **3b** (−2.997 and −3.007 eV, respectively),[13] consistent with the identical potentials for the $\mathbf{1a}^{0/-}$ and $\mathbf{1b}^{0/-}$ couples (−1.11 V vs Fc^+/Fc, Table 1) and with the observation that it is harder to reduce **3a** and **3b** (Table 1). The HOMO for **1a** is 0.11 eV lower than that of **1b** which compares well with the potential of the first oxidation of **1a** being 0.16 V more positive than the first oxidation of **1b**. Similar observations have been made for **3a** and **3b** in which the first oxidation of **3a** is 0.15 V more positive than that of **3b** and for which DFT calculations reveal that the HOMO for **3a** is 0.11 eV lower in energy than that of **3b**.[13] The energies of the HOMOs of **1a** and **1b** (−5.306 and − 5.197 eV, respectively, Figure 5) are ca. 0.05 eV lower than their counterparts in **3a** and **3b** (−5.256 and −5.143 eV, respectively) which is consistent with the result that **1a** and **1b** are harder to oxidize than **3a** and **3b**.

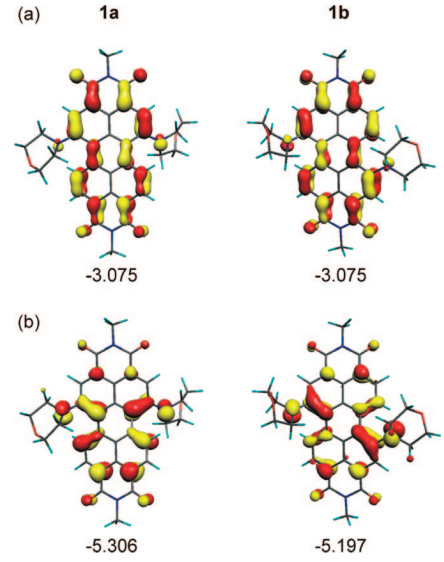

FIGURE 5. Isosufaces at 0.04 e $Å^{-3}$ and energies (eV) for the LUMOs (a) and HOMOs (b) of **1a** and **1b**.

Conclusions

We have prepared and, for the first time, separated the isomers of bis-morpholinyl-substituted perylene bisimides. Electrochemical and spectroelectrochemical investigations of the two isomers reveal contrasting behavior between the two isomers. Although the two isomers exhibit highly similar reduction behavior, as is common for perylene bisimides, the observation and characterization of a two electron oxidation process for the 1,7-isomer, **1b**, is unusual. Indeed the oxidation behavior of **1b** contrasts not only with the corresponding 1,6-isomer, **1a**, but also with the behavior of a related secondary amine-substituted analogue and 1,7-bis(*n*-octylamino)-3,4:9,10-perylenetetracarboxylic acid bisimide **3b**.[13] The contrasting behavior of secondary and tertiary amine substituted perylene bisimides provides significant hope for the fine-tuning of the redox manifold provided by these highly unusual and interesting molecules.

Experimental Section

Synthetic Procedures. Synthesis of *N*,*N*′-Bis(*n*-butyl)-1,6-dimorpholino-3,4:9,10-perylenetetracarboxylic Acid 1a and *N*,*N*-Bis(*n*-butyl)-1,7-dimorpholino-3,4:9,10-perylenetetracarboxylic Acid Bisimide 1b. *N*,*N*′-Di(*n*-butyl)dibromoperylene-3,4,9,10-tetracarboxylic acid bisimide[20] as an approximately 1:4 mixture of 1:6 to 1:7 isomers (550 mg) was dissolved in morpholine (10 cm^3) and stirred at 65 °C for 3 days. After being cooled to room temperature, the mixture was poured into 10% HCl and extracted with CH_2Cl_2. The organic phase was dried over Na_2SO_4, filtered, and concentrated. Purification by column chromatography using CH_2Cl_2 as eluent yielded two major fractions.

1a: blue solid; yield 15%; R_f (CH_2Cl_2) 0.42; ^{1}H NMR ($CDCl_3$) δ 9.88 (d, 2H, J = 8.29 Hz), 8.63 (d, 2H, J = 8.29 Hz), 8.41 (s, 2H), 4.23 (t, 4H), 3.94 (m, 8H), 3.29 (m, 4H, NCH_2, morpholine), 3.12 (m, 4H), 1.75 (m, 4H), 1.50 (m, 4H), 1.01 (t, 6H); ^{13}C NMR ($CDCl_3$) δ 163.6, 152.1, 135.5, 130.8, 128.4, 124.4, 123.8, 123.6, 122.0, 121.6, 121.0, 66.6, 51.8, 40.5, 40.4, 30.3, 20.5, 13.1; MS (MALDI-TOF) m/z 672.3 (M^+); fluorescence emission (CH_2Cl_2) λ_{ex} = 623 nm, λ_{em} = 723, 802 (sh) nm. Anal. Calcd for $C_{40}H_{40}N_4O_6$: C, 71.41; H, 5.99; N, 8.33. Found: C, 71.38; H, 5.93; N, 8.36.

1b: green solid; yield 65%; R_f (CH_2Cl_2) 0.38; ^{1}H NMR ($CDCl_3$) δ 9.73 (d, 2H, J = 8.27 Hz), 8.44 (d, 2H, J = 8.27 Hz), 8.39 (s, 2H), 4.24 (t, 4H), 3.95 (m, 8H), 3.41(m, 4H), 3.19 (m, 4H), 1.76 (m, 4H), 1.47 (m, 4H), 1.02 (t, 6H); ^{13}C NMR ($CDCl_3$) δ 163.5, 163.4, 150.0, 135.1, 130.1, 128.5, 124.7, 123.8, 123.3, 123.0, 121.5, 66.5, 51.5, 40.5, 30.3, 24.9, 20.5, 14.0; MS (MALDI-TOF) m/z 672.3 (M^+); fluorescence emission (CH_2Cl_2) λ_{ex} = 652 nm, λ_{em} = 728, 796 (sh) nm. Anal. Calcd for $C_{40}H_{40}N_4O_6$: C, 71.41; H, 5.99; N, 8.33. Found: C, 71.35; H, 5.89; N, 8.42.

Single-Crystal X-ray Structural Study. Single-crystal X-ray data collection on **1b** was carried out at Station 9.8 of the Daresbury Laboratory Synchrotron Radiation Source, using a wavelength of 0.6911 Å.[21] Further details of structure refinement can be found in the Supporting Information.

Electrochemical and Spectroelectrochemical Measurements. Standard cyclic voltammetry was carried out under an atmosphere of argon using a three-electrode arrangement in a single compartment cell. A glassy carbon working electrode, a Pt wire secondary electrode, and a saturated calomel reference electrode, chemically isolated from the test solution via a bridge tube containing electrolyte solution and fitted with a porous Vycor frit, were used in the cell. The solutions were 10^{-3} M in test compound and 0.4 M in $[NBu_4][BF_4]$[22] as supporting electrolyte. Redox potentials are quoted versus the ferrocenium-ferrocene couple used as an internal reference.[23] Bulk electrolysis experiments, at a controlled potential, were carried out using a two-compartment cell. The Pt/Rh gauze basket working electrode was separated from the wound Pt/Rh gauze secondary electrode by a glass frit. Electrolysed solutions were transferred to quartz tubes, via steel canula, for analysis by EPR spectroscopy. For oxidations, electrolysis and manipulations were performed at or below 243 K.

The UV/vis spectroelectrochemical experiments were carried out with an optically transparent electrochemical (OTE) cell.[24] A three-electrode configuration, consisting a Pt/Rh gauze working electrode, a Pt wire secondary electrode (in a fritted PTFE sleeve) and a saturated calomel electrode, chemically isolated from the test solution via bridge tube containing electrolyte solution and termi-

(20) Chao, C.-C.; Leung, M.; Su, Y. O.; Chiu, K.-Y.; Lin, T.-H.; Shieh, S.-J.; Lin, S.-C. *J. Org. Chem.* **2005**, *70*, 4323.

(21) Cernik, R. J.; Clegg, W.; Catlow, C. R. A.; Bushnell-Wye, G.; Flaherty, J. V.; Greaves, N.; Burrows, I.; Taylor, D. J.; Hamichi, M. *J. Synchrotron Rad.* **1997**, *4*, 279–286.

(22) Kubas, J. *Inorg. Synth.* **1990**, *28*, 68.

(23) Gagné, R. R.; Koval, C. A.; Lisensky, G. C. *Inorg. Chem.* **1980**, *19*, 2854.

(24) Macgregor, S. A.; McInnes, E.; Sorbie,R. J.; Yellowlees, L. J. *Molecular Electrochemistry of Inorganic, Bioinorganic and Organometallic Compounds*; Pombeiro, A. J. L., McCleverty, J. A., Eds.; Kluwer Academic Publishers: New York, 1993; p503.

nated in a porous frit, was used in the cell. For full details of electrochemical and spectroelectrochemical measurements, see Supporting Information.

DFT Calculations. Restricted DFT calculations were performed on models of **1a** and **1b** derived from the X-ray crystal structure of **1b**. The geometry optimizations of the models of **1a** and **1b** were performed without any restraints. The calculations employed the B3LYP functional and the 6-31G* basis set for all atoms, and were performed with Gaussian 03 Revision D. 01.[25]

Acknowledgment. We gratefully acknowledge the support of Engineering and Physical Sciences Research Council (GR/S97521/01 and EP/D048761/1) and the EU through the NANOMESH STRP NMP4-CT-2004-013817 for funding. STFC for the award of beam time on Daresbury SRS Station 9.8.

Supporting Information Available: Full experimental details, original ^{1}H and ^{13}C NMR spectra, and mass spectra for **1a** and **1b**; full UV−vis and EPR data for all the oxidation and reduction processes; further details of DFT calculations. Details of structural refinement and CIF file for **1b**. This material is available free of charge via the Internet at http://pubs.acs.org.

JO801557E

(25) Frisch, M. J.; Trucks, G. W.; Schlegel, H. B.; Scuseria, G. E.; Robb, M. A.; Cheeseman, J. R.; Zakrzewski, V. G.; Montgomery, J. A.; Stratmann, R. E.; Burant, J. C.; Dapprich, S.; Millam, J. M.; Daniels, A. D.; Kudin, K. N.; Strain, M. C.; Farkas, O.; Tomasi, J.; Barone, V.; Cossi, M.; Cammi, R.; Mennucci, B.; Pomelli, C.; Adamo, C.; Clifford, S.; Ochterski, J.; Petersson, G. A.; Ayala, P. Y.; Cui, Q.; Morokuma, K.; Malick, D. K.; Rabuck, A. D.; Raghavachari, K.; Foresman, J. B.; Cioslowski, J.; Ortiz, J. V.; Stefanov, B. B.; Liu, G.; Liashenko, A.; Piskorz, P.; Komaromi, I.; Gomperts, G.; Martin, R. L.; Fox, D. J.; Keith, T.; Al-Laham, M. A.; Peng, C. Y.; Nanayakkara, A.; Gonzalez, C.; Challacombe, M.; Gill, P. M. W.; Johnson, B. G.; Chen, W.; Wong, M. W.; Andres, J. L.; Head-Gordon, M.; Replogle, E. S.; Pople, J. A. *Gaussian 03 Revision D. 01*; Gaussian, Inc., Wallingford CT, 2004.